

Review on Active Galactic Nuclei at hard X-ray energies

L. Bassani^{*a}, M. Molina^a, A. Malizia^a, F. Panessa^b, R. Landi^a, A. Bazzano^b, P. Ubertini^b, A. J. Bird^c and J. B. Stephen^a

^a INAF/IASF Bologna, Italy

^b INAF/IAPS Rome, Italy

^c School of Physics and Astronomy, University of Southampton, UK

E-mail: bassani@iasfbo.inaf.it

Hard X-ray surveys are an important tool for the study of active galactic nuclei (AGN): they provide almost an unbiased view of absorption in the extragalactic population, allow the study of spectral features such as reflection and high energy cut-off which would otherwise be unexplored and favour the discovery of some blazars at high redshift. Here, we present the absorption properties of a large sample of INTEGRAL detected AGN, including an update on the fraction of Compton thick objects. For a sub-sample of 87 sources, which represent a complete set of bright AGN, we will discuss the hard X-ray (20–100 keV) spectral properties, also in conjunction with Swift/BAT 58 month data, providing information on BAT/IBIS cross-calibration constant, average spectral shape and spectral complexity. For this complete sample, we will also present broad-band data using soft X-ray observations, in order to explore the complexity of AGN spectra both at low and high energies and to highlight the variety of shapes. Future prospects for AGN studies with INTEGRAL will also be outlined.

An INTEGRAL view of the high-energy sky (the first 10 years) - 9th INTEGRAL Workshop and celebration of the 10th anniversary of the launch,

October 15-19, 2012

Bibliothèque Nationale de France, Paris, France

*Speaker.

1. Introduction

The study of active galactic nuclei (AGN) above 10 keV is essential if one wants to study non-thermal processes and observe those sources which are strongly affected by absorption in the soft X-ray band. Another advantage is the possibility of having information on spectral features such as the high energy cut-off and the reflection fraction, which cannot be explored with observations performed below 10 keV. The determination of these parameters is important for many reasons: they provide an insight into the physical properties of the region around the central power source, play a key role in synthesis models of the cosmic X-ray background and are important ingredients for unification theories and torus studies (e.g [33, 10, 11]).

2. The sample

In the 4th survey [4] made by INTEGRAL/IBIS [35] there are 234 objects which have been identified with AGN. To this set of objects, one can add 38 galaxies listed in the INTEGRAL all-sky survey by [19] updated on the website¹ but not included in the Bird et al. catalogue due to the different sky coverage. The final dataset comprises 272 AGN (last update March 2011), which represents the most complete view of the INTEGRAL extragalactic sky to date [21]. This sample has two great strengths: a) all sources have optical spectra, which means a secure identification and a measured redshift (the only exception is the BL Lac object RX J0137.7+5814 for which no redshift is available), and b) all sources have X-ray data available, which provides a measure of the source intrinsic absorption. In the left panel of figure 1, the whole sample is reported in the classical 20–100 keV luminosity *vs* redshift plot. The luminosities have been calculated for all sources assuming $H_0=71 \text{ km s}^{-1} \text{ Mpc}^{-1}$ and $q_0 = 0$. From this figure, it can be estimated that our sensitivity limit is around $1.5 \times 10^{-11} \text{ erg cm}^{-2} \text{ s}^{-1}$. We find that the source redshifts span from 0.0014 to 3.7 with a mean at $z=0.1477$, while the Log of 20–100 keV luminosities ranges from 40.7 to ~ 48 with a mean at around $10^{46} \text{ erg s}^{-1}$. NGC 4395 (a Seyfert 2) is the closest and least luminous AGN seen by INTEGRAL, while IGR J22517+2218 (a broad line QSO) is the farthest and most luminous; the former hosts a relatively small central black hole ($M \sim 10^4\text{--}10^5 M_\odot$), while the latter houses a more massive one ($M=10^9 M_\odot$). Thus the INTEGRAL AGN catalogue spans many order of magnitudes in source luminosity and black hole mass, indicating that it covers a large range in Eddington luminosities and accretion rates.

Although useful for statistical and population studies, this catalogue is too large and contains too many weak sources to be appropriate for hard X-ray spectral studies (either individually or in combination with low energy observations). For this purpose we have created a subsample of objects which constitute a complete sample of AGN selected in the 20–40 keV band. Full details on the extraction of this complete sample are given in [20]. It consists of 87 active galaxies of various optical classification: 41 type 1 AGN (Seyfert 1, 1.2 and 1.5), 33 type 2 AGN (Seyfert 1.9 and 2), 5 narrow line Seyfert 1s (NLSy1s) and 8 Blazars (QSOs and BL Lacs). In the right panel of Figure 1, the objects in this subsample are displayed in the 20–100 keV luminosity *vs* redshift plot; it is clear from a comparison between the two panels that the data sets are similar in parameter distribution

¹<http://hea.iki.rssi.ru/integral/survey/catalog.php>

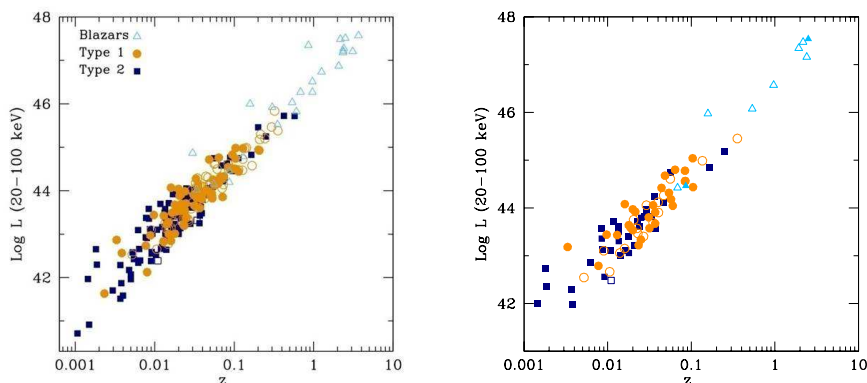


Figure 1: *Left Panel:* Hard X-ray luminosity vs redshift for the INTEGRAL sample of 272 AGN. Circles are type 1 AGN, squares are type 2 AGN and triangles are blazars. Filled symbols represent objects with absorption measured while open symbols refer to sources with upper limits N_{H} . *Right Panel:* Same as in the left panel but using only objects belonging to the complete AGN sample.

so that we can safely assume that the complete sample is representative of the entire population of AGN selected in the hard X-ray band.

3. Absorption properties

In the following, $N_{\text{H}}=10^{22} \text{ cm}^{-2}$ is assumed as the dividing line between absorbed and unabsorbed sources: this is the value conventionally used because it corresponds to a column density sufficiently high to hide an AGN broad line region (BLR, [29]). We also consider as Compton thick an object with a column density in excess of $1.5 \times 10^{24} \text{ cm}^{-2}$. It is worth noting that for a number of objects we did not measure any absorption in excess to the Galactic value and have therefore used the Galactic column density as an upper limit to the source intrinsic absorption. With the assumptions made above, the fraction of absorbed objects present in our sample is 49%, while that of Compton thick objects is around $\sim 6\%$, in full agreement with previous estimates available in the literature ([20], [6]).

Despite the fact that hard X-ray instruments are the least biased in terms of detecting absorbed AGN, they still miss some Compton thick objects, essentially those with weak (intrinsic) fluxes and at large distances. This has been fully discussed by [20] and [6], who have shown that once the correction for this bias is applied, the real intrinsic fraction of Compton-thick AGN is around 20-24%. In particular, in our previous work ([20]) we have adopted a redshift cut ($z=0.015$ or 60 Mpc) in our complete sample of INTEGRAL AGN in order to remove the bias and to probe, although only locally, the entire AGN population. Following this reasoning and using the entire AGN sample, we should be able to expand our previous analysis and to confirm our initial hypothesis, having in mind that the present sample although enlarged is not complete. To allow a comparison with the work of [20], we have divided the sample in the same redshift bins (up to $z=0.57$ considering only those AGN with $\text{Log } L_{20-100\text{keV}} \leq 46$) and plotted the fraction of absorbed ($N_{\text{H}} > 10^{22} \text{ cm}^{-2}$) objects compared to the total number of AGN in these bins. The result is shown in Figure 2 (left

panel), for the enlarged (red points) and complete sample (black points). A number of considerations can be made from this figure. First, the bias in z is still present as we keep observing a trend of decreasing fraction of absorbed objects as the redshift increases. Second, in the first bin the fraction of absorbed objects remains the same as found before: in particular we find that, out of 66 objects, 53 (or 80%) have a column density $\geq 10^{22}$ and 11 (or $17\% \pm 3\%$) are Compton thick. Taking into consideration the fact that the entire sample is not complete, these results are in close agreement with those found previously and confirm the original suggestion that our survey is able to pick up all AGN, even the most absorbed ones, but only in the local Universe. Finally, the fraction of absorbed (and Compton thick) AGN has increased in the second bin from 35% to 57% (including 4 Compton thick sources), implying that as the INTEGRAL survey progresses, we are able to pick up more absorbed objects among those which are distant and faint and therefore lost in previous catalogues.

We thus conclude that the bias affecting deep hard X-ray surveys of AGN is real but negligible if we deal with objects located in the nearby Universe, where the “true” fraction of absorbed and Compton thick objects can be estimated with some precision at 80% and $\sim 17\%$ respectively. Similar indications are now emerging also from X-ray observations of AGN samples selected in other wavebands. For example [5] studied the AGN present in the extended IRAS 12 micron sample [28] for which an XMM-Newton observation is available and found that the fractions of obscured and Compton thick objects are $62 \pm 5\%$ and $20 \pm 4\%$ respectively. [1] presented instead the XMM-Newton spectral analysis of all 38 Seyfert galaxies in the Palomar spectroscopic sample of [15]: they estimate the fraction of absorbed nuclei to be $75 \pm 19\%$, while that of Compton-thick sources to be 15-20%. So the numbers obtained from samples selected in various wavebands seem to converge at least for what concern the local Universe, while at high z the situation is by far less certain.

4. Hard X-ray spectra

One problem effecting the study of the hard X-ray spectra of AGN is the low statistical significance of the data which often limits the measurements of parameters such as the reflection fraction and the high energy cut-off. A way to overcome this problem is to combine data from INTEGRAL/IBIS and Swift/BAT. Before doing so, it is important to cross calibrate the two instruments: one way is the classical method of using the Crab [16], another is to use average spectra of large samples of objects belonging to the same class. About 80 objects of the 87 listed in the complete INTEGRAL sample have also BAT data available from the 58-month survey². A simple power law fit to the combined IBIS/BAT points of all these AGN provides a cross-calibration constant of 1.14 ± 0.04 , sufficiently close to one to justify the joint use of both datasets. The simple power law turns out to be a good description of the 20–100 keV spectra in most cases, with only 35% of the sources requiring a more complex fit. The average photon index is around 2 for the entire sample and for Seyfert 1 and 2 individually; only Blazars display a slightly flatter spectrum ($\Gamma \sim 1.7$). Interestingly this average spectrum (especially considering Seyfert 1 alone) is steeper than that measured in the CAIXA sample of bright type 1 AGN where $\Gamma = 1.73 \pm 0.09$ when reflection is included in the fit [3]; this could be taken as evidence for the presence of a high energy cut-off in

²<http://heasarc.gsfc.nasa.gov/docs/swift/results/bs58mon/>

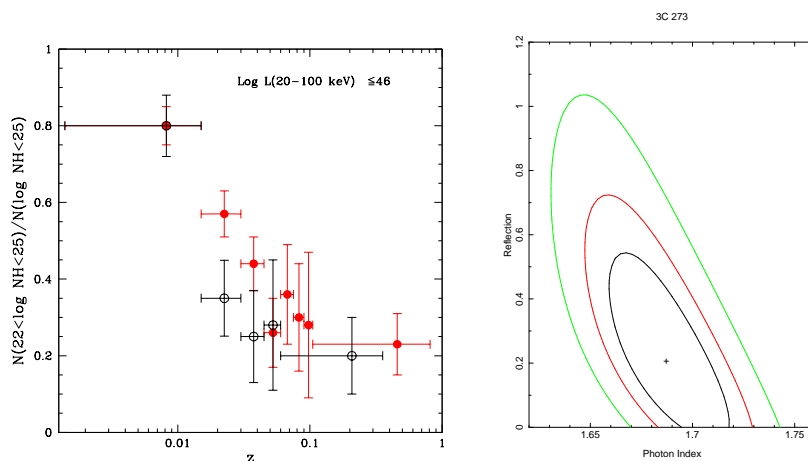


Figure 2: *Left Panel:* Fraction of absorbed objects compared to the total number of AGN as a function of redshift from enlarged (red points,[21]) and complete (black points,[20]) samples respectively. *Right Panel:* `pexrav` model applied to the combined IBIS/BAT data of 3C 273 with the high energy cut-off fixed to 1 MeV.

the IBIS/BAT waveband. The presence of this (and the reflection) component can be tested via the `pexrav` model applied to those sources where a simple power law is not a good fit to the data; although the improvement is significant in most cases, good constraints on all spectral parameters are obtained only for NGC 4151 and IC 4329A. This indicates that, if one wants to get some spectral information from the hard X-ray spectra alone, some assumptions must be made on at least one of the 3 parameters involved in the spectral analysis (photon index, cut-off energy and reflection). For example in IGR J21247+5058, if we fix the reflection to zero as found by [22, 32], the photon index and the cut-off energy can be well constrained ($\Gamma=1.7^{+0.1}_{-0.1}$ and $E_c=155^{+71}_{-37}$ keV) and provide values compatible with previous studies. On the other hand, if in the Circinus Galaxy the high energy cut-off is set to be around 50 keV as measured in the past (e.g. [34]), the photon index and the reflection can be estimated with some precision ($\Gamma=1.80^{+0.03}_{-0.03}$ and $R=0.59^{+0.29}_{-0.24}$). Finally in the case of 3C 273, where the cut-off is known to be around 1 MeV, the reflection component can be constrained to be below 0.3 (see Figure 2, right panel). Unfortunately, such assumptions are not possible in all cases and so one has to rely on broad-band data to obtain more stringent constraints on source parameters.

5. Broad-band analysis

A further step towards the comprehension of hard X-ray selected AGN properties is provided by broad-band X-ray studies. In a series of papers [23, 24, 25, 9], we have combined IBIS spectra with data obtained at soft X-ray energies by various satellites such as XMM-Newton, Swift, Chandra etc., to obtain information on various spectral features for most AGN in the complete sample. Here, we report a compendium of the results obtained in these papers. A first result is the great variety in shapes observed and the extreme complexity found when modelling most sources; many spectral components have to be considered, although they are not present all the time with similar strength. The soft excess for example is observed in a good fraction of Seyfert 1, but dominates

dominates only in few of these AGN; it is always present in Seyfert 2, but in 6 objects has a more complex shape than a simple scattered power law. Absorption is measured in all type 2 objects, while complex absorption is found in 25% of type 1 sources: in this last case one or more layers of absorbing material partially covering the source are often found. The average photon index is typically 1.7, flatter than the canonical value measured in the hard X-ray band but compatible with that measured in the CAIXA sample. Figure 3 shows the photon index distribution obtained for type 1 and type 2 AGN separately: the two distributions as well as the average Γ (1.74, $\sigma=0.2$ and 1.68, $\sigma=0.3$ for Seyfert 1 and 2 respectively) are very similar, which immediately suggests that the production mechanism is the same in both types of AGN.

Although high energy spectral components (reflection and the high energy cut-off) are not easy to measure due to the sources spectral complexity and non simultaneity of the soft and hard X-ray data, they have nevertheless being measured in a number of objects. As is evident in figure 3 (right panel), the distribution of measured cut off energies clusters around 100 keV while the bulk of the lower limits on this parameter are found below 300 keV. One must then conclude that high energy cut-off is present and cannot be ignored (as often happens) in broad band fits. This result is in line with a number of previous studies [26, 8, 2] but is only barely consistent with those obtained by [27], who locate the cut-off energy above 200-300 keV. We also note that our result is in line with the synthesis models of the cosmic diffuse background (CXB) which often assume an upper limit of ~ 200 keV for the AGN mean cut-off energy. This choice is basically driven by the intensity and shape of the CXB spectrum above the peak, which cannot be exceeded; even a value of 300 keV has difficulties in accommodating all available observations and CXB measurements [14].

Finally, Figure 3 (left and right panels) shows a compendium of the results obtained for the reflection component in both type 1 and type 2 AGN; note that R is linked to the solid angle Ω as $R=\Omega/2\pi$ and that measured values and upper limits are shown separately in the figure. The distributions of R are similar in both types as well as the average reflection values; it is also evident that large values of R are found in highly variable sources and simply reflect the limitation due to the use of non simultaneous data.

6. Future prospects and conclusions

The number of AGN selected in the hard X-ray band is continuously increasing thanks to both the INTEGRAL and Swift surveys and many of the initial expectations have been fulfilled but also many questions have been raised by the observations made so far. Probably the shift in the next few years will be to multi-waveband studies of these objects which provide an alternative view due to their hard X-ray selection: overall IBIS/BAT objects are less affected by absorption than sources selected in other wavebands and are representative of the population of high luminosity AGN. Thus multiwaveband studies of them can provide new clues on how AGN work. For example, by combining radio and hard X-ray information on a well defined sample of AGN, one can study the jet-disk connection in supermassive black holes (Panessa et al. these proceedings) or test if jets are made by e^+e^- pairs [13]. Also by surveying hard X-ray selected AGN for water maser emission, one can expect to probe the physics of accretion disks, especially in those AGN which are often obscured at optical/UV and even X-ray wavelengths by large column densities of gas and dust along the line of sight [7]. Already the discovery of a water maser feature in the nucleus of

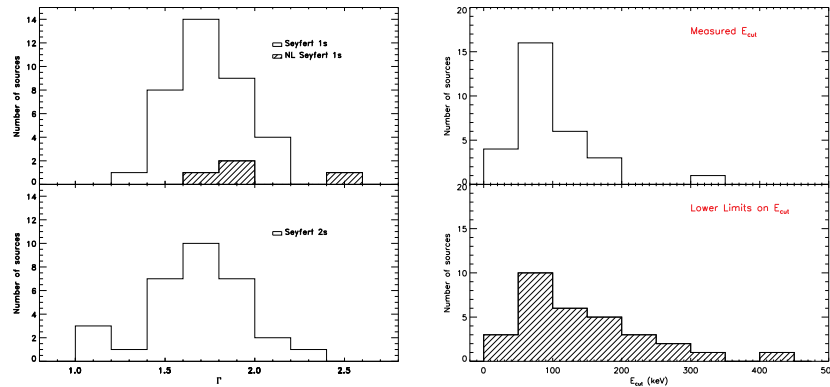


Figure 3: Left Panel: Distribution of photon indices of Seyfert 1 (including Narrow Line Seyfert1) at the top and Seyfert 2 at the bottom, as obtained from broad band X-ray data. Right Panel: Distribution of cut off energies (measured values at the top and lower limits at the bottom) for the complete sample of AGN as obtained from broad band X-ray data.

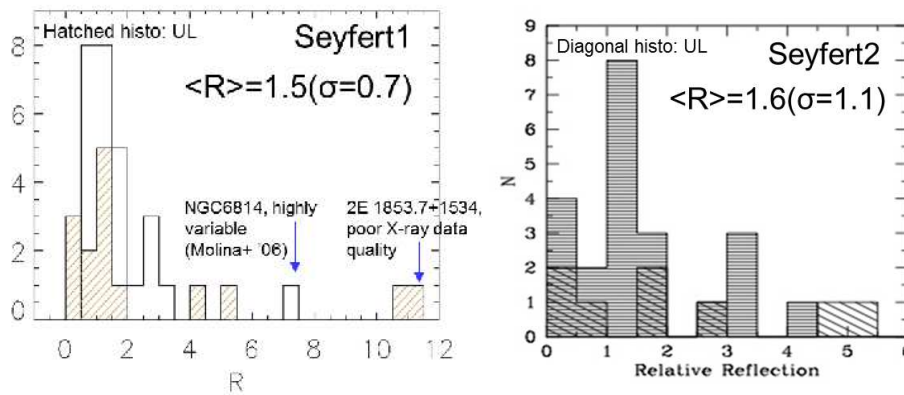


Figure 4: Left Panel: Distribution of the reflection component R for the Seyfert 1 in the complete sample as obtained from broad band X-ray data; upper limits on R are shown as a diagonal histogram. Right Panel: Same as in left panel but for Seyfert 2.

IGR J16385-2057 has opened a new field of maser studies in Narrow Lines Seyfert 1 galaxies and highlighted the possibility of detecting this emission in elliptical galaxies [30, 31]. As underlined by [11], modelling of the infrared spectra of a complete sample of hard X-ray selected AGN can provide the only way to measure the intrinsic distribution of torus covering factors and thus provide the ultimate test for the clumpy torus model. Finally, one should note that BAT/IBIS samples of AGN show a large fraction (20-30%, [17]) of systems in interaction, mergers, dual objects etc. Combined radio/optical/X-ray observations of these systems offer a unique opportunity to study AGN activation (see for example [18]), probe the relation between interaction and absorption and ultimately understand how black holes grow.

This is of course only the beginning of hard X-ray studies of AGN, since INTEGRAL is approved up to 2014 and hopefully beyond, Swift/BAT is still in orbit and performing well and Nustar has just joined the group with great expectations, but as Plato would say “The beginning is the most important part of the work”.

References

- [1] Akylas A. & Georgantopoulos I., 2009, *A&A*, 500, 999
- [2] Beckmann V., Soldi S., Ricci C. et al. 2009, *A&A*, 505, 417
- [3] Bianchi S., Guainazzi M., Matt G. et al., 2009, *A&A*, 495, 421
- [4] Bird A.J., Bazzano A., Bassani L. et al., 2010, *ApJS*, 186, 1
- [5] Brightman M. & Nandra K., 2011, *MNRAS*, 413, 1206
- [6] Burlon D., Ajello M., Greiner J. et al., 2011, *ApJ*, 728, 58
- [7] Castangia P., Tarchi A., Panessa F. et al., 2011, *Extremesky 2011*
- [8] Dadina M. 2008, *A&A*, 485, 417
- [9] De Rosa A., Panessa F., Bassani L. et al., 2012, *MNRAS*, 420, 2087
- [10] Elitzur M. & Shlosman I., 2006, *ApJL*, 648, 101
- [11] Elitzur M., 2012, *ApJL*, 747, 33
- [12] Filippenko A. V. & Ho L. C., 2003, *ApJL*, 588, 13
- [13] Ghisellini G. 2012, *MNRAS*, 424, 26
- [14] Gilli R., Comastri A. & Hasinger G. 2007, *A&A*, 463, 79
- [15] Ho L. C., Filippenko A. V., Sargent W. L. et al., 1997, *AAS*, 189, 122.09
- [16] Kirsch M. G. et al., 2005, *SPIE*, 5898, 22
- [17] Koss M., Mushotzky R., Veilleux S., Winter L., 2010, *ApJ* 746, 22
- [18] Koss M., Mushotzky R., Treister E. et al., 2012, *ApJ*, 716, 125
- [19] Krivonos R., Revnivtsev M., Lutovinov A. et al., 2007, *A&A*, 475, 775
- [20] Malizia A., Stephen J. B., Bassani L. et al., 2009, *MNRAS*, 399, 944
- [21] Malizia A., Bassani L., Bazzano A. et al. 2012, *MNRAS*, 426, 1750
- [22] Molina M., Giroletti M., Malizia A. et al., 2007, *MNRAS*, 382, 937
- [23] Molina M., Bassani L., Malizia A. et al., 2009, *MNRAS*, 399, 1293
- [24] Panessa F., Bassani L., de Rosa A. et al. 2008, *A&A*, 483, 151
- [25] Panessa F., de Rosa A., Bassani L. et al. 2011, *MNRAS*, 417, 2426
- [26] Perola G. C., Matt G., Cappi M. et al., 2002, *A&A*, 389, 802
- [27] Ricci C., Walter R., Courvoisier T. J.-L. et al., 2011, *A&A*, 532, 102
- [28] Rush B., Malkan M. A. Spinoglio L., 1993, *ApJS*, 89, 1
- [29] Silverman J. D., Green P. J., Barkhouse W. A. et al., 2005, *ApJ*, 618, 123
- [30] Tarchi A., Castangia P., Henkel C. et al., 2011, *A&A*, 525, 91
- [31] Tarchi A., Castangia P., Columbano A. et al., 2011, *A&A*, 532, 125
- [32] Tazaki F., Ueda Y., Ishino Y. et al., 2010, *ApJ*, 721, 1340
- [33] Urry C. M. & Padovani P., 1995, *PASP*, 107, 803
- [34] Yang Y., Wilson A. S., Matt G. et al., 2009, *ApJ*, 691, 131
- [35] Winkler C., Courvoisier T.J.L., Di Cocco G., et al., 2003, *A&A*, 411, L1